

# Gas detection with quantum cascade lasers: An adapted photoacoustic sensor based on Helmholtz resonance

Stefano Barbieri,<sup>a)</sup> Jean-Paul Pellaux, Eric Studemann, and Daniel Rosset  
*Orbisphere, CH-1222 Vésenaz-Genève, Switzerland*

(Received 27 December 2001; accepted for publication 3 February 2002)

A photoacoustic gas sensor exploiting a quantum cascade laser as a radiation source is demonstrated. A detection limit of  $\sim 1$  ppm with 1 ms response time is found using a Peltier-cooled Fabry–Pérot InGaAs-based quantum cascade laser emitting at  $9.4 \mu\text{m}$ , and a commercial microphone as a detector. The photoacoustic cell consists of a Helmholtz resonator preceded by a low-pass acoustic filter. This geometry is well adapted to the shape of the laser beam and allows for an effective filtering of ambient acoustical noise. The relative simplicity of the system is particularly attractive for applications where sensitivity, robustness, and ease of fabrication are all fundamental requirements. © 2002 American Institute of Physics. [DOI: 10.1063/1.1480463]

## I. INTRODUCTION

Diode lasers (DL's) represent the ideal sources for application to *in situ* optical gas sensing. Among their most useful properties, the possibility of electrically tuning the emission wavelength has allowed for the introduction of a whole family of wavelength modulation techniques which, during the last few years, considerably improved the sensitivity, selectivity, and response time of optical gas detectors.<sup>1</sup> Also, from the point of view of commercial applications, their reduced size and low cost are two fundamental features making DL's particularly competitive with respect to gas lasers and other types of solid-state lasers.

Up until a few years ago, DL's did not provide adequate performance, i.e., single mode emission with output powers in the mW range at room temperature, in the midinfrared (MIR) region of the electromagnetic spectrum. This represented a major limitation to the ultimate sensitivity and selectivity of gas sensors since most molecules have their more intense absorption lines and specific spectral shape in this wavelength range. Indeed, beyond  $\sim 2.5 \mu\text{m}$  wavelength, the only DL's available were lead salt lasers ( $3\text{--}30 \mu\text{m}$ ) which suffer from low output powers and operation at cryogenic temperatures.<sup>2,3</sup> Recently, a new class of solid-state lasers has emerged providing output powers in the mW range together with close to and room-temperature operation. Quantum cascade lasers (QCL's) are semiconductor lasers which rely on intersubband rather than interband transitions as with conventional DL's.<sup>4–6</sup> Thanks to this, devices can be designed with an emission wavelength within the  $3\text{--}25 \mu\text{m}$  range, therefore virtually spanning the whole MIR spectrum.<sup>7</sup>

Applying QCL's to gas sensing, parts per billion (ppb) and sub-ppb detection limits could be reached, therefore proving the potentialities of this new type of source.<sup>8–10</sup> However, such elevated sensitivities were obtained via relatively exotic spectroscopic solutions such as multipass cells

providing hundreds of meters of optical path length, or cavity ringdown spectroscopy. Due to their high cost and complexity, we believe that in spite of their performance, these systems will hardly satisfy market needs except in some particular *niche* applications.

For a couple of decades, laser photoacoustic spectroscopy (LPAS) has emerged as a valid alternative to all-optical spectroscopic techniques, and sub-ppb detection limits are now obtained in commercial systems for trace gas applications.<sup>11–14</sup> In LPAS, the intensity (or the wavelength) of the laser source is modulated at a frequency  $\nu_m$  lying in the acoustic range. A heat transfer occurs from the optically excited molecules to the surrounding ones producing a pressure wave of frequency  $\nu_m$ , which is detected by means of an acoustic transducer. The use of a simple commercial microphone as a detection element constitutes a great advantage of LPAS with respect to transmission spectroscopy techniques. This is particularly relevant when MIR sources are employed. In fact, in this case, nitrogen cooled HgCdTe infrared detectors provide the only viable solution for reaching the required sensitivities, in spite of being expensive and impractical. This is the reason why, although limits of detection in the part per million (ppm) and sub-ppm range were demonstrated with QCL's in standard transmission configurations,<sup>15</sup> nevertheless, it is not clear whether these solutions will ever compete against systems exploiting near IR DL's.<sup>1</sup>

In this article, we present the operation of a gas sensor prototype based on the photoacoustic effect, exploiting a QCL as a radiation source. The main guideline driving the conception of the sensor was that of maximizing its simplicity while keeping a reasonable sensitivity. Previous works demonstrated photoacoustic spectroscopy with QCL's by exciting the fundamental longitudinal acoustic mode of a cylindrical chamber.<sup>16,17</sup> In fact, up to one order of magnitude larger  $Q$  factors could be obtained in a configuration exploiting the resonance of radial modes.<sup>12</sup> Unfortunately QCL's suffer from strong beam divergence, which hinders the possibility of an efficient excitation of such modes.<sup>18</sup> This is the

<sup>a)</sup>Electronic mail: stefano.barbieri@teraview.co.uk

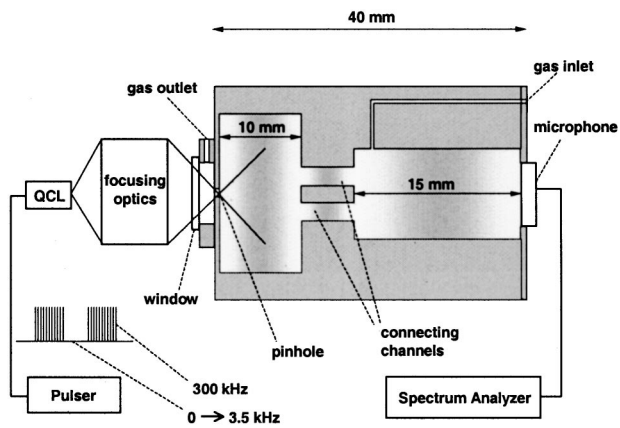


FIG. 1. Schematic drawing of the photoacoustic cell and of the experimental setup. Diameters of first and second cylindrical chamber are 30 mm and 20 mm, respectively, while the interconnecting channels are 10 mm in length and have a diameter of 6 mm. The length of the second chamber can be varied from 20 to 2 mm and the diameter of the pinhole from 5 to 0.5 mm (see text and Figs. 2 and 3). The photoacoustic cell is made of brass and internal surfaces were polished in order to maximize the reflection of radiation. The QCL was driven in pulsed mode (Alpes Lasers Laser Driver 100) with 80 ns pulsewidth and 300 kHz repetition rate. A further slow modulation in the kHz range was added to generate the photoacoustic signal. Gas was introduced in the cell via the back-side inlet channel and could flow out through the short channel close to the ZnSe window (the thickness of the volume beside the window is 0.5 mm). Shaded regions represent pictorially the propagation of the pressure wave that is generated in the first chamber.

reason why here we have chosen to develop a Helmholtz resonator. Compared to the excitation of longitudinal modes, this solution represents an alternative that is particularly well adapted to the shape of QCL's beam. Since we were not particularly concerned with selectivity, all measurements were performed using a multimode emission Fabry-Pérot QCL that was amplitude modulated.

## II. DESIGN OF THE PHOTOACOUSTIC CELL AND EXPERIMENTAL RESULTS

Figure 1 shows the experimental setup together with the schematic drawing of the photoacoustic cell. This consists of a first chamber connected via two 6 mm diameter channels to a second chamber containing the detection microphone. The second chamber plus the connecting channels form a Helmholtz resonator.<sup>12,19–22</sup> This type of resonator does not rely on the generation of standing wave modes.<sup>16,17</sup> Instead, sound amplification is obtained (via left to right oscillations of the gas volume inside the channels. These oscillations generate a periodical compression and expansion of the gas enclosed in the chamber. At resonance, this produces an enhancement of the average pressure inside the chamber with respect to the pressure in the connecting channels. In this instance, the geometrical parameters were selected in order to obtain a resonant frequency  $\nu_0$  in the kHz range.<sup>19</sup>

In the middle of the outer side of the photoacoustic cell (Fig. 1), a 500  $\mu\text{m}$  diameter pinhole is drilled so that the first chamber is terminated on both sides by two openings. This produces a low-pass acoustic filter which attenuates ambient noise as well as window noise generated by radiation absorption in the window which closes the cell.<sup>12,19</sup> By a suitable

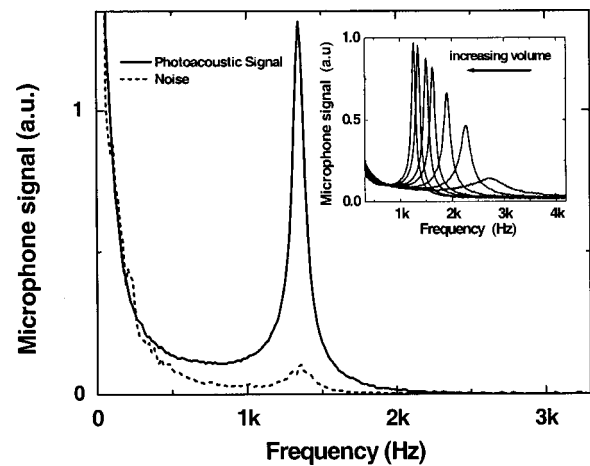


FIG. 2. Photoacoustic and noise spectra of the cell measured by means of a spectrum analyzer (Stanford SR760 FFT). Solid line: Photoacoustic response obtained by filling the cell with ethanol vapors (see Ref. 24) and sweeping the slow modulation frequency from 0 to 3.5 kHz. The length of the inner chamber was set to  $\sim 15$  mm. Dashed line: Noise spectrum obtained by integrating the microphone signal for a few minutes with the QCL switched off. Inset: Photoacoustic spectra obtained by increasing the length of the Helmholtz resonator from  $\sim 2$  to  $\sim 20$  mm.

design, the cutoff frequency of this filter was set at  $\sim 200$  Hz, i.e., well below the resonant frequency of the inner Helmholtz resonator.

The operating principle of the photoacoustic sensor is the following. By electrically modulating the amplitude of QCL radiation at  $\nu_0$  and by focusing the laser beam on the pinhole, we generate a sound wave inside the first volume. This wave enters into the connecting channels giving rise to forced pressure oscillations that are amplified by the Helmholtz resonator and finally detected by the microphone. Therefore, while strongly attenuating environmental and window noise, the low-pass filter does not affect the photoacoustically generated sound wave since this is created *inside* the first chamber. This way, the present cell design allows for an effective increase of the signal to noise ratio.<sup>22</sup> Furthermore, this photoacoustic cell adapts particularly well to sources with strongly divergent beams. In fact, a beam with a wide aperture will excite a maximum gas volume in the first cavity as well as directly inside the channels (Fig. 1).

A multimode Fabry-Pérot InGaAs-based QCL (Alpes Lasers S1838) with a spectral bandwidth of  $\sim 30$   $\text{cm}^{-1}$  centered around an emission wavelength of 9.4  $\mu\text{m}$ , was employed to obtain the frequency response of the present gas sensor (Fig. 2). We used ethanol vapors as absorbing gas.<sup>23,24</sup> The device was mounted on a custom made Peltier cooling system and operated in pulsed mode with 80 ns pulsewidth and 300 kHz repetition rate at a temperature of 240 K. We measured a few mW of average power. A further slow amplitude modulation in the kHz range was superimposed to the fast one, resulting in a train of pulses. This slow frequency was continuously swept between 1 Hz and  $\sim 3.5$  kHz. QCL laser radiation was collected and then refocused on the 500  $\mu\text{m}$  pinhole (Fig. 1) by means of two ZnSe lenses ( $f/0.5$  and  $f/2$ , respectively). The acoustic signal was finally collected by means of a Sennheiser Elektret microphone, model KE

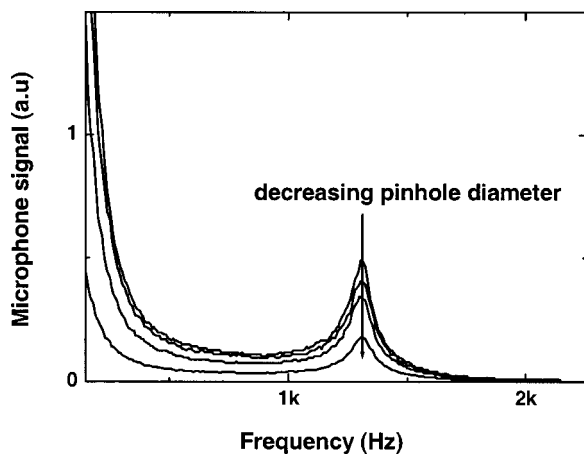


FIG. 3. Noise spectra for different diameters of the pinhole drilled in front of the first volume (Fig. 1). From upper to lower curve, diameters sizes are 5 mm, 3 mm, 1 mm, and 0.5 mm respectively. On the left-hand side, we clearly observe a decrease of the cutoff frequency of the acoustic filter for decreasing hole diameter. A global reduction of the noise intensity is also reported thanks to progressive isolation from external environment.

13-227, and fed into a spectrum analyzer. Measurements were performed with a continuous gas flow.

The pronounced peak at 1.3 kHz in the solid curve of Fig. 2 is due to the Helmholtz resonator, while on the low-frequency side, we clearly observe the effect of low-pass acoustic filtering. The  $Q$  factor of the cavity is obtained from the ratio  $(v_0/\Delta v)$ , where  $v_0$  is the resonance frequency and  $\Delta v$  is the width of the peak at  $1/\sqrt{2}$  of the maximum.<sup>25</sup> From Fig. 2, we obtain  $Q=24$  which is in agreement with calculations.<sup>19</sup> This represents the pressure amplification of our resonator, i.e., the ratio of the acoustic pressure amplitude within the cavity to the driving pressure amplitude inside the channels. The dashed curve of Fig. 2 represents the noise spectrum, obtained by integrating the microphone signal over several minutes with the QCL switched off. By comparison with the solid curve (curves were normalized in order to obtain the same values at low frequencies), we have a clear demonstration of the effect of the acoustic filtering: external noise at 1.3 kHz is reduced while the photoacoustic signal is left unaltered. Similar measurements were performed on a cell consisting of a simple Helmholtz cavity. As expected, in that case, both photoacoustic and noise spectra showed a pronounced peak at the resonant frequency, resulting in a factor of 10 lower signal to noise than that obtained with low-pass filtering. In the inset of Fig. 2, we report the photoacoustic spectra for different volumes of the Helmholtz resonator. The  $Q$  factor increases by a factor of  $\sim 5$  with increasing volume, i.e., by decreasing the resonant frequency from 2.7 to 1.3 kHz [for a simple Helmholtz resonator  $Q$  is proportional to  $(v)^{-1}$ ].<sup>19</sup> In the same frequency range, the noise intensity at resonance was found to increase only by a factor of 3 due to the effect of the acoustic filter. Therefore, by setting the resonant frequency at  $\sim 1.3$  kHz, we optimize the performance of the cell.

In Fig. 3, we report the noise spectrum of the resonator as a function of the diameter of the pinhole drilled in front of the acoustic filter (Fig. 2). As expected, decreasing the hole diameter from 5 to 0.5 mm has two major consequences: (i)

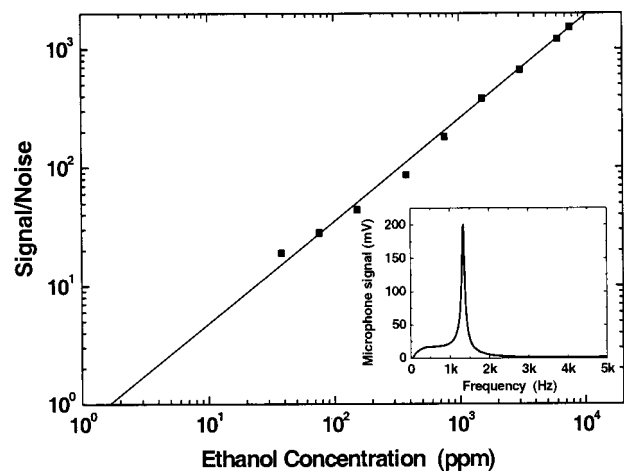


FIG. 4. Signal to noise vs ethanol vapors concentration in ppm. Linear extrapolation leads to  $\sim 1$  ppm minimum detectable concentration. Data was collected with a continuous gas flow. Microphone signal was preamplified and measured with a lock-in amplifier (Stanford SR530) locked at 1.34 kHz (10 ms integration time). This frequency corresponds to the peak of the photoacoustic spectrum shown in the inset. Inset: Photoacoustic spectrum. Filtering of the preamplifier is responsible for the rapid decrease of the signal at low frequencies (compare with Fig. 1).

cutoff frequency is shifted toward lower frequencies, and (ii) the *overall* noise level is substantially reduced due to a more effective acoustic isolation. To this extent, it is to be noted that due to the lateral dimensions of the QCL,  $\sim 30 \times 5 \mu\text{m}$ , the size of the diameter could be further reduced to at least  $\sim 100 \mu\text{m}$  without any power loss. On the other hand, a compromise can be found between the need for a sufficiently low noise level and the size of the pinhole. In fact, considering the beam divergence of the QCL,<sup>18</sup> a hole with a few mm in diameter is sufficient to collect all the emitted radiation when the laser is positioned just in front of the ZnSe window (see Fig. 1). With such a solution, one could eliminate the focusing optics. This would have a clear advantage in terms of lower costs, but also in terms of lower power loss due to reflections at interfaces.

Finally, we evaluated the detection limit of our sensor. This is reported in Fig. 4, which shows the dependence of the measured signal to noise for decreasing ethanol concentration. The laser was operated in pulsed mode as described herein with a slow modulation frequency  $v_m = 1.3$  kHz (see inset). We measured a collected average output power of  $\sim 10$  mW over a single train of pulses ( $T=240$  K). The microphone output signal was fed into a lock-in amplifier after passing through a filtering and preamplification stage.

Over the measured range of concentrations the Beer-Lambert law can be linearized and this explains the observed linear decrease of the photoacoustic signal.<sup>12</sup> The extrapolated minimum detectable concentration is  $\sim 1$  ppm and is limited by electrical pickup noise. The sensitivity obtained is comparable to that reported in Ref. 16 with 1 s integration time. Here, we want to stress that data points were acquired with only 10 ms integration time. In fact, the response time, thanks to the small volume of the cell and the magnitude of  $v_m$ , is below 1 ms.

The present performance shows that the sensor is potentially interesting for a variety of applications ranging from

industrial process control to pollution monitoring. However, we believe that the sensitivity of the sensor can still be improved. Toward this end, the following critical points will be addressed in the future: (i) reduction of electrical pick-up noise, (ii) reduction of acoustic noise, and (iii) increase of cavity  $Q$  factor. Furthermore, the possibility of completely eliminating the optics while still maintaining an effective noise filtering is an option that we are exploring experimentally. With respect to photoacoustic detection schemes based on the excitation of longitudinal modes, which need a focused beam,<sup>16,17</sup> this would represent a considerable advantage in terms of simplicity and ease of fabrication. These results were obtained using a multimode Fabry–Pérot QCL. Actually, the use of DFB devices, which are commercially available, would greatly improve the selectivity of the sensor for applications where spectral interference is a major concern.

### ACKNOWLEDGMENTS

The authors gratefully acknowledge Alpes Laser SA for providing laser drive electronics. This work has been partially funded by the European Community under the Brite/Euram “UNISEL” research project (Contract No. CT97-0557).

<sup>1</sup>P. Werle, *Recent Res. Dev. Opt. Eng.* **2**, 143 (1999).

<sup>2</sup>M. Tacke, *Infrared Phys. Technol.* **34**, 447 (1995).

<sup>3</sup>M. Hodges and U. W. Shiessl, *Proc. SPIE* **3628**, 113 (1999).

<sup>4</sup>J. Faist, F. Capasso, C. Sirtori, D. Sivco, and A. Cho, *Intersubband Transitions in Quantum Wells: Physics and Device Applications II*, edited by H. Liu and F. Capasso (Academic, New York, 2000), Vol. 66, Chap. 1, pp. 1–83; F. Capasso, C. Gmachl, D. L. Sivco, and A. Y. Cho, *Phys. World* **12**, 27 (1999).

<sup>5</sup>J. Faist, M. Beck, T. Aellen, and E. Gini, *Appl. Phys. Lett.* **78**, 147 (2001).

<sup>6</sup>H. Page, C. Becker, A. Robertson, G. Glastre, V. Ortiz, and C. Sirtori, *Appl. Phys. Lett.* **78**, 3529 (2001).

<sup>7</sup>R. Colombelli, F. Capasso, C. Gmachl, A. L. Hutchinson, D. L. Sivco, A.

Tredicucci, M. C. Wanke, A. M. Sergent, and A. Y. Cho, *Appl. Phys. Lett.* **78**, 2620 (2001).

<sup>8</sup>M. S. Zahniser, (Proceedings of the Quantum Cascade Laser Workshop, Freiburg, Germany, February 2001).

<sup>9</sup>A. Kosterev, R. F. Curl, F. K. Tittel, C. Gmachl, F. Capasso, D. L. Sivco, J. N. Baillargeon, A. L. Hutchinson, and A. Y. Cho, *Opt. Lett.* **24**, 1762 (1999).

<sup>10</sup>A. Kosterev, A. Malinovsky, F. K. Tittel, C. Gmachl, F. Capasso, D. L. Sivco, J. N. Baillargeon, A. L. Hutchinson, and A. Y. Cho, *Appl. Opt.* **40**, 5522 (2001).

<sup>11</sup>A. Tam, *Rev. Mod. Phys.* **58**, 381 (1986).

<sup>12</sup>V. P. Zharov and V. S. Letokhov, *Laser Photoacoustic Spectroscopy* (Springer, Berlin, 1986).

<sup>13</sup>S. E. Bialkowski, *Photothermal Spectroscopy Methods for Chemical Analysis* (Wiley, New York, 1996).

<sup>14</sup>Omnisens product data sheet, Trace gas analyzer for ammonia monitoring (Omnisens 2000/Issue 1, 2001).

<sup>15</sup>K. Namjou, S. Cai, E. A. Whittaker, J. Fist, C. Gmachl, F. Capasso, D. L. Sivco, and A. Y. Cho, *Opt. Lett.* **23**, 219 (1998).

<sup>16</sup>B. A. Paldus, T. G. Spence, R. N. Zare, J. Oomens, F. J. M. Harren, D. H. Parker, C. Gmachl, F. Capasso, D. L. Sivco, J. N. Baillargeon, A. L. Hutchinson, and A. Y. Cho, *Opt. Lett.* **24**, 178 (1999).

<sup>17</sup>D. Hofstetter, M. Beck, J. Faist, M. Nägele, and M. W. Sigrist, *Opt. Lett.* **26**, 887 (2001).

<sup>18</sup>S. Schilt, L. Thévenaz, and P. Robert, *IEEE J. Quantum Electron* (unpublished); C. Sirtori, H. Page, C. Becker, and V. Ortiz, *IEEE J. Quantum Electron* (unpublished).

<sup>19</sup>L. E. Kinsler, A. R. Frey, A. B. Coppens, and J. V. Sanders, *Fundamentals of Acoustics* (Wiley, New York, 2000); D. T. Blackstock, *Fundamentals of Physical Acoustics* (Wiley, New York, 2000).

<sup>20</sup>O. Nordhaus and J. Pelzl, *Appl. Phys.* **25**, 221 (1981).

<sup>21</sup>R. Kästle and M. W. Sigrist, *Appl. Phys. B: Lasers Opt.* **63**, 389 (1996).

<sup>22</sup>V. Zeninari, V. A. Kapitanov, D. Courtois, and Y. N. Ponomarev, *Infrared Phys. Technol.* **40**, 1 (1999).

<sup>23</sup>Considering the acoustic filter and the Helmholtz resonator as two independent elements is an approximation. The detailed analysis of the acoustics of the system goes beyond the scope of this work and does not add any valuable insight to the understanding of the operating principle.

<sup>24</sup>Ethanol vapors IR spectrum presents a broad absorption band centered around 9.4  $\mu\text{m}$ .

<sup>25</sup>The  $Q$  factor is defined as the ratio between the resonant frequency and the full width at half maximum of the power spectrum. In Fig. 2, the microphone signal is proportional to pressure therefore the width of the peak must be taken at the  $1/\sqrt{2}$  points of the maximum.